CHEMISTRY OF MATERIALS
Cite This: Chem. Mater. 2018, 30, 2965−2972
Article
pubs.acs.org/cm

Role of Disorder Induced by Doping on the Thermoelectric Properties of Semiconducting Polymers

Elayne M. Thomas,[‡] Bhooshan C. Popere,[§,⊥] Haiyu Fang,[§] Michael L. Chabinyc,*[,‡] and Rachel A. Segalman*[,‡,§]

[‡]Materials Department, University of California, Santa Barbara, Santa Barbara, California 93106, United States
[§]Department of Chemical Engineering, University of California, Santa Barbara, Santa Barbara, California 93106, United States

Supporting Information

ABSTRACT: A fundamental understanding of charge transport in polymeric semiconductors requires knowledge of how the electrical conductivity varies with carrier density. The thermopower of semiconducting polymers is also a complex function of carrier density making it difficult to assess structure−property relationships for the thermoelectric power factor. We examined the thermoelectric properties of poly[2,5-bis(3-tetradecylthiophen-2-yl)thieno[3,2-*b*]thiophene] (pBTTT-C_{14}) by measurements of an electrochemical transistor using a polymeric ionic liquid (PIL) gate dielectric that can modulate the carrier concentration from 4×10^{18} to 3×10^{20} cm^{-3}. As carrier density increases, so does the concentration of associated counterions, leading to a greater degree of energetic disorder within the semiconductor. Using thermopower measurements, we show experimentally that the electronic density-of-states broadens with increasing carrier density in the semiconducting polymer. The origin of a commonly observed power law relationship between thermopower and electrical conductivity is discussed and related to the changes in the electronic density-of-states upon doping.

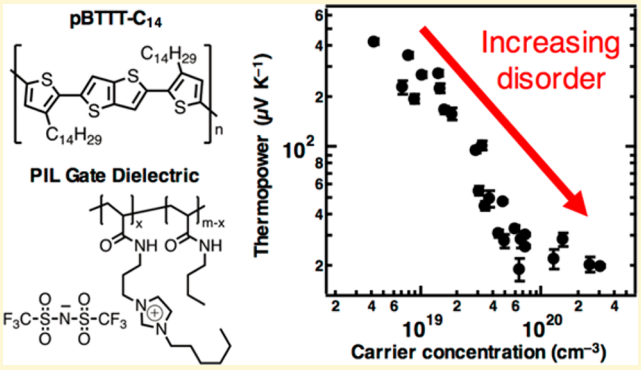

INTRODUCTION

Doping is an important process for controlling the electrical properties of semiconductors.[1] In contrast to the substitution of atomic donors or acceptors into inorganic semiconductors, a common method to modify the carrier concentration in semiconducting polymers is to introduce electron-deficient (or electron-rich) molecules, usually from solution or from the vapor phase, to oxidize (or reduce) the polymer backbone.[2,3] In this case, the dopant molecule, now ionized, is the counterion to the charged backbone. Protonating the polymer backbone with a Brönsted acid provides a similar effect with the proton donor acting as the counterion.[4] Alternatively, electrochemical methods can be used to supply or remove electrons but frequently require the polymer to be supported on a conductive substrate. Addition of dopants, or counterions, can increase the concentration of charge carriers in the polymer but concomitantly increase energetic disorder within the material due to structural perturbations.

Emerging applications for semiconducting polymers including thermoelectrics[5] and bioelectronics[6] rely on tuning the conductivity by either molecular or electrochemical doping. Here, we examine how changes in the electronic density-of-states (DOS) of a semiconducting polymer occur during electrochemical doping. By using an electrochemical transistor (OECT), we measured the changes in conductivity and thermopower of poly[2,5-bis(3-tetradecylthiophen-2-yl)thieno[3,2-*b*]thiophene] (pBTTT-C_{14}) as a function of carrier concentration. Controlling charge density provides a way to develop robust transport models for doped organic semiconductors and guide new materials design.

Studying the thermoelectric behavior in semiconducting polymers is one route to understand their transport properties and changes in the DOS upon doping. The carrier concentration, p, contributes to the physical properties of the semiconductor that determine its thermoelectric performance, including thermopower (α), electrical conductivity (σ), and thermal conductivity (κ). The general equation for thermopower is defined in eq 1 where $df(E)/dE = -f(E)(1 - f(E))/k_BT$ is the derivative of the Fermi−Dirac function $f(E)$, E_F is the Fermi energy, and $\sigma(E)$ is a transport function of electrical conductivity with energy.

$$\alpha = -\frac{k_B}{e}\int \frac{E - E_F}{k_BT}\frac{\sigma(E)}{\sigma}\frac{df(E)}{dE}dE \quad (1)$$

If transport is mostly dominated by carriers around the Fermi level, thermopower can be rewritten as eq 2.[7]

Received: January 26, 2018
Revised: April 9, 2018
Published: April 23, 2018

DOI: 10.1021/acs.chemmater.8b00394
Chem. Mater. 2018, 30, 2965−2972

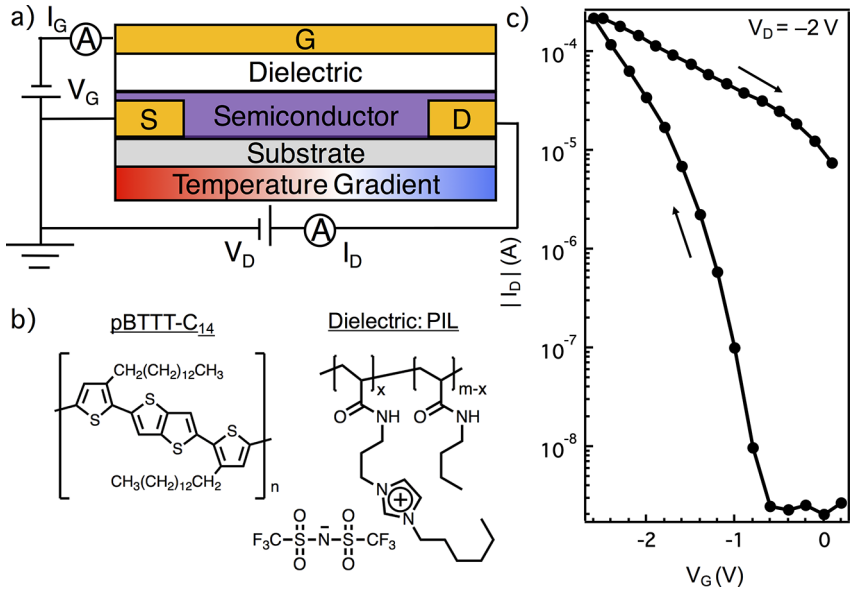

Figure 1. (a) Schematic representation of the TGBC OFET structure used for thermoelectric and electrical measurements. (b) Chemical structures of the polymeric ionic liquid (PIL) and p-type semiconductor (pBTTT-C_{14}) used in this work; $x = 0.9$. (c) PIL transistor transfer curve using a scan rate of 3.3 mV s^{-1}.

$$\alpha = \frac{\pi^2}{3}\frac{k_B^2 T}{e}\left\{\frac{d(\ln\sigma(E))}{dE}\right\}_{E=E_F} \quad (2)$$

The sign and magnitude of thermopower is determined by the slope of $\ln(\sigma(E))$ at the Fermi level, which in turn is dependent on the occupancy of the electronic density-of-states.[7] Thermopower measurements are therefore an experimental method to ascertain the Fermi level if the functional form for $\sigma(E)$ is known.

The electrical conductivity of semiconducting polymers is a complex function of the carrier concentration due to energetic disorder.[8−10] The majority of current transport models for semiconducting polymers use a hopping model with a density-of-states based on either a Gaussian function or a Mott-type model with a free-electron gas form combined with an exponential tail of states below a mobility edge.[11,12] For both of these models, the carrier density is required to rationalize transport data. Measuring the carrier concentration in doped polymers is notoriously difficult due to the emergence of bipolarons, which are silent in EPR,[13] and the energetic disorder present in many polymers, which makes interpretation of Hall effect measurements challenging.[14] A method to experimentally determine carrier density is thus imperative to evaluate transport models in disordered systems.

Field-effect gating controls carrier density in a semiconductor by applying biases to the terminal of a transistor.[15] An advantage of field-effect gating is quantification of the total charge induced in the semiconductor, p, and the ease of changing it experimentally. In transistors, carriers are induced in the semiconductor in a thin, ∼2 nm, conducting channel at the interface between the semiconductor and dielectric.[16] More recently, ion-containing gate dielectrics have been used to dope semiconductors through an electrical double layer or electrochemically by allowing ions in the dielectric to infiltrate the semiconductor layer.[17] Infiltration of ions into the active layer permits a 3D active channel of charge carriers rather than a channel only at the dielectric−semiconductor interface. As a result, the range of carrier density differs between the two devices. The maximum carrier density using conventional dielectrics, such as SiO_2, approach 10^{19} cm^{-3} above which dielectric breakdown occurs from the applied field, while electrochemical transistors have accessed carrier densities approaching 10^{21} cm^{-3}.[14,18,19] This broad range of carrier density can probe transport behavior over a wide range of doping levels from where traps may dominate (<∼10^{19} cm^{-3}) to concentrations where extended state conduction may occur.

Herein, we employ a polymeric ionic liquid (PIL) as the gate dielectric to investigate thermoelectric transport of a p-type semiconductor in an OECT geometry. To eliminate unwanted ion-pair diffusion into the semiconducting layer, a single-ion conducting PIL restricts ion motion to one species by tethering one ion to the polymer backbone. This unique OECT architecture therefore provides a model system to study the influence of doping on thermoelectric charge transport over a large range of carrier density. We find that high doping levels induce significant broadening in the polymer density-of-states, signifying that a balance exists between high electrical conductivity and a well-ordered electronic structure.

RESULTS AND DISCUSSION

A PIL-Gated Transistor Provides Controllable Carrier Concentration for Thermoelectric Transport. Gated measurements allow for the study of both thermopower and electrical conductivity of a material.[19−21] The device structure and materials examined here are shown in Figure 1. The p-type semiconducting polymer, pBTTT-C_{14} (Figure 1a), was chosen as the active layer due to its high carrier mobility in thin film transistors (∼1 cm^2 V^{-1} s^{-1}).[22,23] An aprotic PIL was used as the gate dielectric with an imidazolium-based cation, denoted IM^+, on the main chain and bis(trifluoromethane)sulfonimide ($TFSI^-$) as the free anion (Figure 1a). In many ionic liquid-gated transistors, an ionic liquid is blended with a host polymer allowing both the cation and anion to be mobile.[24] Polyelectrolyte gate dielectrics, typically with a proton as the cation, can only p-dope the semiconductor interfacially which limits the range of achievable carrier concentration.[25,26] With

DOI: 10.1021/acs.chemmater.8b00394
Chem. Mater. 2018, 30, 2965−2972

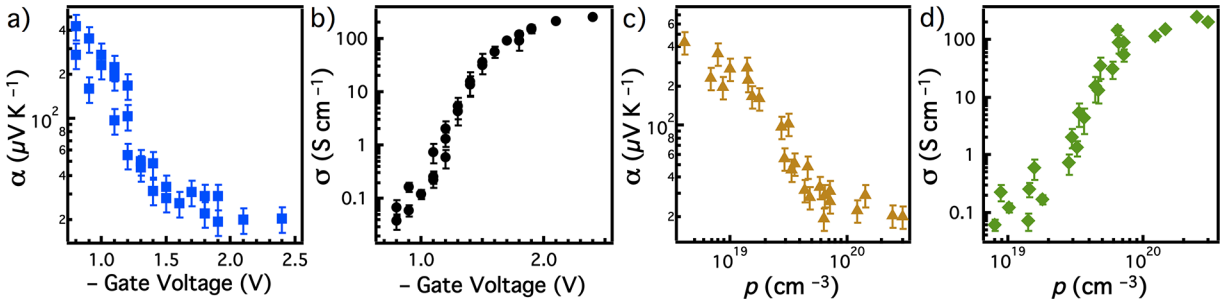

Figure 2. (a) Thermopower and (b) electrical conductivity measured over the range of gate voltages used. (c) Thermopower and (d) electrical conductivity as a function of carrier concentration calculated through integrating gate current.

the PIL, the cation is covalently linked the polymer backbone and immobile, while $TFSI^-$ is mobile and acts as the counterion to holes induced in the bulk of the semiconductor. Dielectric spectroscopy measurements show that the IM-TFSI PIL exhibits maximum capacitance of around 1 μF cm^{-2} at low frequencies (Figure S1), comparable to an IL with the same ionic species.[27] A high-capacitance dielectric allows for a large concentration of charge to be induced without the need to apply large biases; a block copolymer PIL synthesized previously[28] exhibited a maximum capacitance of 3 μF cm^{-2} and threshold voltage of −0.75 V in a transistor.

The basic characteristics of the PIL-gated transistor are similar to IL-gated transistors (Figure 1b). As a negative bias between source and gate (V_G) is applied, the device acts similar to a capacitor, where charge builds up at both interfaces of the dielectric. Holes are injected into the semiconducting layer from the source electrode, whose charge is then compensated by $TFSI^-$ from the PIL dielectric. Tracking the current generated (I_G) with time determines the total charge generated in the semiconductor (Q). Carrier concentration is calculated by eq 3, where A is the area of charge accumulation and t is the thickness of the accumulation layer.[29]

$$p = \frac{Q}{V_G} = \frac{\int I_G - I_L dt}{eAt} \tag{3}$$

In this work, it is assumed that the semiconductor volume remains constant during gating. Previous work has shown that infiltration of external molecules can perturb the crystalline domains of the semiconductor, as observed by an ∼10% increase in the alkyl stacking direction and decrease in π–π stacking distance at high dopant concentration.[2,30] As there is no direct method available to measure polymer swelling as a function of gate bias in this work, we take this as a possible source of a small systematic error.

Charges induced in the semiconductor generate a current between source and drain, I_D, as a source-drain bias (V_D) is applied. Drain current is linearly proportional to V_D at low bias (i.e., the "linear regime"), with the slope related to the semiconductor resistance. The transfer characteristics of the PIL-gated transistor in Figure 1c show that the device turns ON at approximately −0.6 V, consistent with the high capacitance of the dielectric. Hysteresis between forward and backward sweeps in the transfer curve is also observed in Figure 1c, which is commonly seen in devices with ion-based gate dielectrics.[31]

The PIL gate provides a means to control thermopower and electrical conductivity over a large range of carrier concentration, shown in Figure 2. Because the PIL capacitance is frequency dependent, it is important that measurements reflect the relevant time scales of ion motion; ultimately, the steady-state properties of the semiconductor are of interest rather than sweep-rate dependent characteristics. As a result, a protocol to verify the measurement was carried out at steady state was used (see Experimental Section and Supporting Information). As the transistor turns ON, holes are injected from the source electrode along with $TFSI^-$ ions diffusing from the PIL dielectric to act as the countercharge. Higher bias leads to more occupied states in the semiconductor, thus increasing the doping level. As a result, larger bias leads to smaller thermopower as carrier concentration increases. On the basis of the crystallographic unit cell, we estimate a maximum number of states of approximately 2.0 × 10^{21} cm^{-3} in pBTTT, assuming each monomer can contribute 2 electrons.[16] The maximum calculated carrier density from the PIL is 3 × 10^{20} cm^{-3}, corresponding to 0.3 charges per monomer. Incorporating a maximal swelling of the semiconductor layer upon ion infiltration introduces an error of approximately 10% for carrier concentration at the highest carrier densities. The ability to modulate the carrier concentration from 10^{18} to greater than 10^{20} cm^{-3} has been observed previously using ion gels and ionic liquids as gate dielectrics;[14,20] in this work, constraining the cation to remain in the dielectric ensures that one induced charge corresponds to only one additional ion within the semiconductor. This range of carrier density gives rise to a broad window to explore transport phenomena while maintaining control over Fermi level in the semiconductor.

We measured both α and σ over the accessible range of p to determine the relationship between the three parameters. As carrier concentration increases, electrical conductivity increases and plateaus around 200 S cm^{-1} while the thermopower decreases followed by a similar plateau. Rather than changing sign, the minimum thermopower of ∼20 μV K^{-1} occurs at approximately −1.5 V, meaning that the slope $d(\ln(\sigma(E)))/dE$ remains positive for all values of carrier concentration (eq 2). These values are relatively consistent with studies of pBTTT that modulate α and α through acid doping in solution[2] and ion gel gating.[20] However, carrier concentration must be known to truly compare thermopower values between samples. Conductivity normally acts as a proxy for carrier concentration, but film processing conditions can affect conductivity for a given carrier concentration which enables a range of conductivity values for a given value of the Seebeck coefficient.[5]

Predictive Models for Density-of-States Indicate Broadening in the High Carrier Concentration Limit. With the knowledge of the conductivity and thermopower, we can apply models previously used to interpret the thermopower of doped semiconducting polymers. One model developed by Emin and co-workers for polaronic species combines entropic

DOI: 10.1021/acs.chemmater.8b00394
Chem. Mater. 2018, 30, 2965−2972

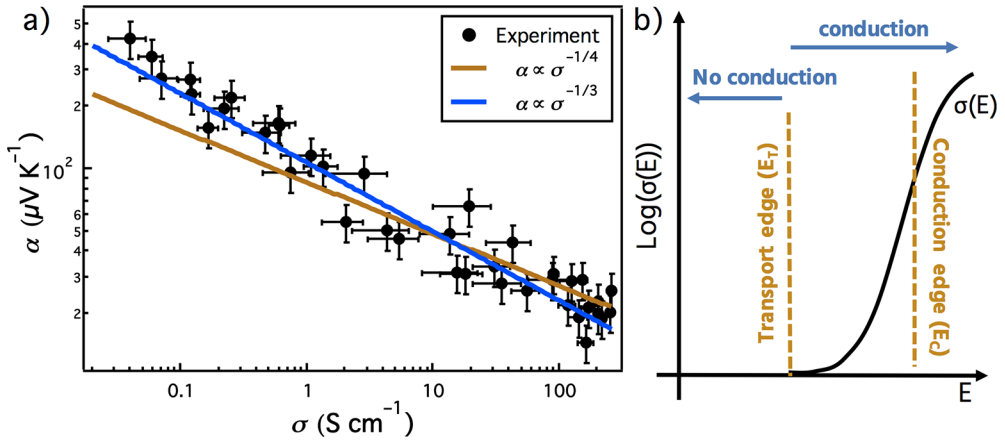

Figure 3. (a) Double logarithm plot of thermopower with electrical conductivity. Two power law fits are presented, with power exponents of −1/3 (blue) and −1/4 (orange). Error in thermopower is the standard ±20% to account for errors in temperature measurement. For the $\alpha \propto \sigma^{-1/3}$ fit, σ_{E0} = 0.002 S cm^{-1}. (b) Schematic demonstrating the difference between the transport edge E_T and the more traditional conduction or "mobility" edge, E_C, where extended state conduction occurs. In the Kang and Snyder model, conduction can occur below E_C but not below the transport edge.

and vibronic contributions of carriers to the thermopower described in eq 4 to account for entropy of mixing (N is the total number of sites; n is the occupied number of sites), spin degeneracy, and effects of polarons on molecular vibrations (α_{vib}).[16]

$$\alpha = \frac{k_B}{e}\ln\left(\frac{N-n}{n}\right) + \frac{k_B}{e}\ln(2) + \alpha_{vib} \quad (4)$$

This formalism has been used for previous work in field-effect transistors but is only valid when $n \ll N$, the maximum number of thermally accessible states, which does not strictly apply for the range examined here (Figure S2).

Others have turned to electrical conductivity as a proxy for p in conventional doping methods when carrier concentration is difficult to measure. A multitude of semiconducting polymers exhibit a power law trend between thermopower and conductivity, which was observed in previous studies and was fit empirically to $\alpha \propto \sigma^{-1/4}$ in recent work.[32,33]

A recent formalism developed by Kang and Snyder defined a transport function, σ_E, to further explain the α–σ relationship.[34] The transport function is described in eq 5, where σ_{E0} is a transport coefficient that is dependent on temperature but independent of energy and s is the transport parameter. E_T is the transport "edge", below which no conduction is expected to occur.

$$\sigma_E(E, T) = \sigma_{E0}(T)\left(\frac{E - E_T}{k_B T}\right)^s \quad (5)$$

E_T is different from a Mott-like mobility edge E_C, because Mott's model assumes extended state transport only above E_C rather than the possibility of hopping conduction above E_T in the Kang and Snyder model. In the degenerate limit relative to the transport edge, the thermopower can be defined in terms of conductivity, the transport parameter, and the transport coefficient from eq 6, leading to a scaling law of $\alpha \propto \sigma^{-1/s}$ for heavily doped polymers.

$$\alpha = \frac{k_B}{e}\frac{\pi^2}{3}s\left(\frac{\sigma}{\sigma_{E0}}\right)^{-1/s} \quad (6)$$

The value of s is currently not predictable by the model and is a parameter chosen to fit experimental data.

Due to the ability to vary electrical conductivity and thermopower via gating, we can access the relationship between conductivity and thermopower and also both as a function of the carrier concentration. The scaling relationship is clearly observed from Figure 3 over a wide range of known carrier concentration. The α–σ power law trend from this work is best fit with a slope of −1/3 (blue trace); a slope of −1/4 is also shown in comparison, which fits reasonably well to the higher conductivity data but deviates below $\sigma \approx 1$ S cm^{-1}.

The degree of control attained by varying gate bias also modulates the Fermi level over a large energy range. Using eq 6 with s = 3, reduced chemical potential ($\eta = \frac{E_F - E_T}{k_B T}$) was calculated for each experimental value of α to track E_F with respect to the transport edge. In the limit of high thermopower, E_F lies below E_T (i.e., $\eta < 0$), while at low thermopower the Fermi level extends to more than 1 eV past E_T (Figure S3). In the semiconductor degenerate limit, eq 3 reduces to eq 7.

$$\alpha = \frac{k_B}{e}\frac{\pi^2}{3}s\eta^{-1} \quad (7)$$

The degenerate approximation becomes valid when $\eta = \sim 8$ or when $\alpha = \sim 100$ μV K^{-1} from Figure S3. As a result, the $\alpha \propto \sigma^{-1/3}$ relationship should only be valid for $\alpha < 100$ μV K^{-1} but seems to reasonably fit the entire data range.

We can consider the physical significance of the parameters in light of our experimental system. Our data shows an energetic difference of 1 eV between E_F and the transport edge at high carrier concentration. This value is relatively large; although the exact bandwidth of semiconducting polymers is unknown, DFT calculations of models of ideal infinite crystals gives a bandwidth along the backbone and π-stacking direction around 0.67 and ∼ 1eV for pBTTT, respectively.[35,36] These models do not account for any local distortions from oxidation of the backbone, i.e., polaron formation. Additionally, the assumption of a static transport model is unlikely, particularly in the limit of high carrier concentration where ions infiltrate into the semiconductor. Therefore, it is imperative to consider a nonstatic density-of-states to understand the origin of seemingly large values of η at the highly doped limit.

The Kang and Snyder model provides a direct connection between thermopower and Fermi level relative to E_T using the transport function. To better connect these results with

DOI: 10.1021/acs.chemmater.8b00394
Chem. Mater. 2018, 30, 2965−2972

experimental values, one must understand how gating affects the density-of-states. This has been notoriously difficult in organic semiconductors due to disorder and nonuniform microstructure.[37] One of the most common formalisms was developed by Mott and Davis where $\sigma(E)$ is calculated for a conduction or "mobility" edge, E_C, given by eq 8 where $\mu(E)$ is defined as *microscopic* mobility, the carrier mobility for a given energy level.[7]

$$\sigma(E) = \begin{cases} \mu(E)eN(E)k_BT, & E > E_C \\ 0, & E \leq E_C \end{cases} \quad (8)$$

The microscopic mobility is not equivalent to the macroscopic mobility measured experimentally because an experimental value is averaged over all accessible energies.

Although utilized in literature for disordered materials such as amorphous silicon, eq 8 holds true only for a specific functional form of the conductivity function. From the Kubo-Greenwood formalism, Cohen et al. derive a more general relationship.[38] From the definition of electrical conductivity, Cohen et al. find eq 9 assuming independent carriers which is a more general form than eq 8.

$$\frac{d\sigma(E)}{dE} = e\mu(E)N(E) \quad (9)$$

A more detailed derivation may be found in the Supporting Information. From the goodness-of-fit for $s = 3$ in Figure 3, it is evident that $\sigma \propto E^3$ (eq 2). The right side of eq 9 must therefore scale with energy to the power of $(s - 1) = 2$. Although density-of-states and microscopic mobility are not completely disentangled in eq 6, it allows us to examine cases between these parameters to make reasonable predictions for carrier transport. While they do not consider hopping explicitly, their formalism can still be used with the assumptions here.

The carrier concentration can be used to verify that the parameters used in the fits of the transport data are reasonable. Carrier density is related to the density-of-states through the Fermi–Dirac function, shown in eq 10.

$$p = \int N(E)(1 - f(E, E_F))\, dE \quad (10)$$

We can first model the DOS assuming it is constant with doping via $N(E) = N_0 \times (E - E_T)^m$, where m dictates the DOS dependence on energy. This functional form for $N(E)$ is not intuitive a priori but is a direct result of the fit in Figure 3 and the transport function in eq 5. Here, the prefactor, N_0, is chosen such that all models converge to the same point at 1 eV above the transport edge, above which the functional form of the conductivity function cannot be predicted (Supporting Information). Assuming this form, it follows that $\mu(E) = \mu_0 \times (E - E_T)^{2-m}$ to be consistent with eq 9. Three values of m were used to compare with experimental values: $m = 1/2$, $m = 1$, and $m = 2$. The former is similar to a free-electron gas model of the DOS in inorganic semiconductors, and the latter tests the validity of an energy-independent mobility, i.e., a constant mobility for the states above E_T. The carrier density is simulated as a function of E_F using eq 10 and compared to carrier density values attained experimentally.

Use of a static DOS fails to reproduce experimental carrier concentration with respect to the Fermi level (Figure 4). The successful fit of $\alpha \propto \sigma^{-1/3}$ combined with eqs 5 and 7 substantiates the use of a power-law DOS function assuming a constant mobility, but a constant DOS may oversimplify actual

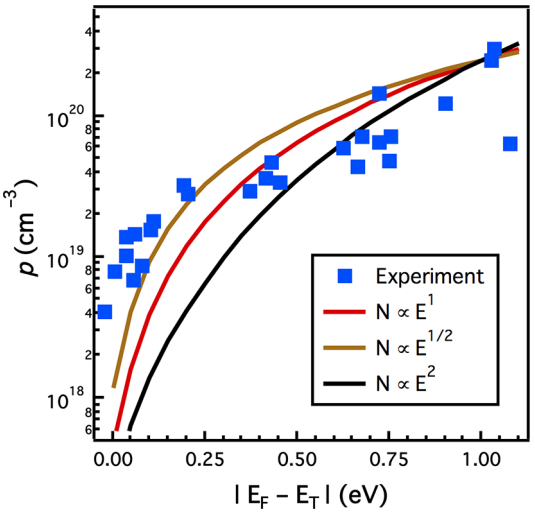

Figure 4. Carrier concentration measured experimentally (blue squares) compared to simulated carrier density for three power-law DOS models. The power-law form shown is for a DOS function that is static with doping.

transport behavior. The assumption of constant mobility is plausible at energies above the conduction edge, but the functional form of $\mu(E)$ is less clear near the transport edge. The density-of-states and $\mu(E)$ could be changing in tandem, but we only consider the former since $\mu(E)$ cannot be measured experimentally.

A dynamic DOS shape in organic semiconductors has been considered in previous work through modeling a Gaussian density-of-states as well as an exponential form.[8,9,39] It is possible, then, that (1) the energy dependence of the DOS is changing with E_F (i.e., m is changing along with the functional form of the mobility) or (2) the prefactor, N_0, is changing with E_F. Here, N_0 gauges the slope of the density-of-states. Since thermopower is determined by carriers near the Fermi level, N_0 only reflects the local slope of the DOS around E_F.

Using eq 10, we can calculate the value of N_0 necessary for each model to match carrier concentration measured at each energy assuming a constant mobility. Figure 5a shows that, for all models, N_0 decreases as E_F shifts farther from the transport edge. As N_0 decreases, the slope of the density-of-states at the Fermi level becomes shallower, indicating that the local DOS shape is broadening (Figure 5b). The most likely cause of this broadening is disorder induced by incorporation of the $TFSI^-$

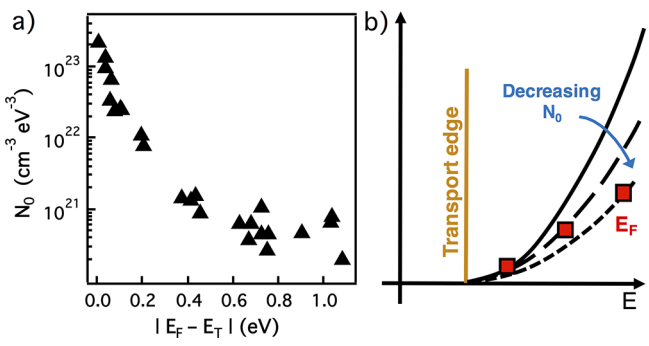

Figure 5. (a) Variation of the DOS prefactor, N_0, with energy; representative data is shown for $m = 2$. (b) Schematic of evolution of DOS with increasing doping, where the Fermi level moves further past the transport edge as carrier concentration increases.

DOI: 10.1021/acs.chemmater.8b00394
Chem. Mater. 2018, 30, 2965–2972

counterions as the carrier concentration increases. Doping-induced energetic disorder in organic materials was first modeled by Arkhipov et al.[9] and theoretically connected to thermopower by Abdalla et al. using a modified Gaussian density-of-states that incorporates Coulombic interactions of ionic dopants.[40] Using this formalism, the $\alpha-\sigma$ power law trend was found to hold over a relatively wide range of conductivities substantiating the importance of incorporating energetic disorder into transport models for doped polymeric semiconductors.

As previously mentioned, introducing small molecules to dope the semiconductor has been shown to perturb the physical structure at high dopant concentration,[2,41−43] which concomitantly changes the electronic landscape. Similar results have been shown using PPV[44] and more recently P3HT[45] through temperature-dependent measurements using a Gaussian form of the DOS. For a given temperature, a steeper DOS at the Fermi level leads to higher thermopower from eq 2. As a result, increasing carrier concentration reduces thermopower not only from the reduction in entropy per carrier but also through decreasing the slope of $N(E)$ through electronic disorder. A balance therefore exists in polymeric semiconductors to increase carrier concentration while minimizing perturbation in the density-of-states, which is affected by molecules infiltrating the material.

CONCLUSIONS

We have studied the thermoelectric properties of a semicrystalline polymer by using a PIL as the gate dielectric in a transistor architecture. A clear power law trend in thermopower and electrical conductivity is observed across 4 orders of magnitude in σ, revealed through controlling carrier density with gate bias. Modeling the data with a power-law density-of-states shows that a static function does not fit the experimental trend in carrier concentration with energy. In considering a power-law DOS function that varies with carrier concentration, we observe a decrease in the density-of-states prefactor, N_0, with increasing carrier density. This suggests that the local slope of the DOS decreases and energetic disorder increases as E_F moves past the transport edge.

The formalism used here implies that mobility may also be a function of energy for a given Fermi level. Understanding if and how the functional form of $\mu(E)$ would change with carrier concentration remains a subject for future studies. While we cannot directly probe $\mu(E)$, as experimentally measured mobility values are averaged over all energies, we expect that the microscopic mobility would become relatively independent of energy at high carrier concentration.

Changes observed in the semiconductor energetic landscape raise questions as to the effects of ion infiltration on the polymer microstructure.[46,47] Connecting microstructural changes with thermoelectric properties may offer more insight into a unifying model for charge transport in semiconducting polymers. Designing new semiconducting polymer−ion combinations to minimize structural changes could reduce perturbations in the DOS, leading to new limits in high-performance polymeric thermoelectrics.

EXPERIMENTAL SECTION

Materials. pBTTT-C_{14} was synthesized using a literature procedure.[48] All solvents were anhydrous and purchased from Sigma-Aldrich. Gold foil for top gates was purchased from Alfa Aesar. The IM-TFSI PIL was synthesized via reversible addition-fragmentation chain-transfer (RAFT) polymerization, with the detailed synthetic scheme in the Supporting Information.

Device Fabrication. Top-gate bottom-contact thin film transistors were fabricated in a nitrogen filled glovebox. Source and drain electrodes (20 nm Au) were thermally evaporated on glass substrates using a shadow mask. Channel lengths varied between 100 and 150 μm, and channel widths were 2700 μm. A solution of pBTTT-C_{14} (5 mg/mL, chlorobenzene) was spuncast at 1000 rpm for 1 min and annealed at 180 °C for 10 min affording a film thickness of approximately 25 nm as measured by atomic force microscopy. A PIL solution (50 mg/mL, acetonitrile) was dropcast in a PDMS mold to cover the semiconducting channels and annealed under vacuum at 70 °C overnight. Once annealed, the mold was removed to access the gold contacts. Gold foil was placed on top of the annealed PIL to act as the gate electrode.

Thermopower Metrology. The device geometry used in this work necessitated a protocol to measure S, σ, and n in the same experiment. To compensate for slow ion diffusion, measurements began several minutes after applying a gate bias. Thermopower was obtained by applying a series of four temperature differences between the source and drain; the resulting voltage was recorded. Electrical conductivity was calculated from resistance measurements. Carrier concentration was calculated using eq 2, where the full semiconductor thickness was used as a conservative estimate of n. Thus, each gate bias yielded a set of values for the thermoelectric properties of interest. More detail regarding the protocol is found in Figure S3.

ASSOCIATED CONTENT

Supporting Information

The Supporting Information is available free of charge on the ACS Publications website at DOI: 10.1021/acs.chemmater.8b00394.

PIL synthetic details and frequency-dependent capacitance, comparison of Emin model for thermopower, calculated reduced chemical potential from Kang and Snyder model, gated measurement experimental protocol, derivation of eq 9 in main text, full form of power law equations used for carrier concentration fits (PDF)

AUTHOR INFORMATION

ORCID

Elayne M. Thomas: 0000-0003-0072-4204
Michael L. Chabinyc: 0000-0003-4641-3508
Rachel A. Segalman: 0000-0002-4292-5103

Present Address

[⊥]The Dow Chemical Company, 455 Forest Street, Marlborough, MA, 01752.

Notes

The authors declare no competing financial interest.

ACKNOWLEDGMENTS

The authors gratefully acknowledge support from the Department of Energy Office of Basic Energy Sciences under Grant No. DE-SC0016390. E.M.T. kindly acknowledges a National Science Foundation Graduate Research Fellowship under Award No. 1650114. Synthesis of the PIL was supported by the Air Force Office of Scientific Research through the Multidisciplinary University Research Initiative on Controlling Thermal and Electrical Transport in Organic and Hybrid Materials, Grant No. AFOSR FA95501210002, and measurements under shared facilities were supported through the MRSEC Program of the National Science Foundation under Award DMR-1720256.

DOI: 10.1021/acs.chemmater.8b00394
Chem. Mater. 2018, 30, 2965−2972

REFERENCES

(1) Jacobs, I. E.; Moule, A. J. Controlling Molecular Doping in Organic Semiconductors. *Adv. Mater.* **2017**, *29*, 1703063.

(2) Patel, S. N.; Glaudell, A. M.; Kiefer, D.; Chabinyc, M. L. Increasing the Thermoelectric Power Factor of a Semiconducting Polymer by Doping from the Vapor Phase. *ACS Macro Lett.* **2016**, *5*, 268−272.

(3) Yim, K. H.; Whiting, G. L.; Murphy, C. E.; Halls, J. J. M.; Burroughes, J. H.; Friend, R. H.; Kim, J. S. Controlling electrical properties of conjugated polymers via a solution-based p-type doping. *Adv. Mater.* **2008**, *20*, 3319−3324.

(4) Han, C. C.; Elsenbaumer, R. L. Protonic Acids - Generally Applicable Dopants for Conducting Polymers. *Synth. Met.* **1989**, *30*, 123−131.

(5) Patel, S. N.; Glaudell, A. M.; Peterson, K. A.; Thomas, E. M.; O'Hara, K. A.; Lim, E.; Chabinyc, M. L. Morphology controls the thermoelectric power factor of a doped semiconducting polymer. *Sci. Adv.* **2017**, *3*, e1700434.

(6) Khodagholy, D.; Doublet, T.; Quilichini, P.; Gurfinkel, M.; Leleux, P.; Ghestem, A.; Ismailova, E.; Herve, T.; Sanaur, S.; Bernard, C.; Malliaras, G. G. In vivo recordings of brain activity using organic transistors. *Nat. Commun.* **2013**, *4*, 1575.

(7) Mott, N. F.; Davis, E. A. *Electronic Processes in Non-Crystalline Materials*, 2 ed.; Oxford University Press: New York, 1979.

(8) Zuo, G. Z.; Li, Z. J.; Andersson, O.; Abdalla, H.; Wang, E. G.; Kemerink, M. Molecular Doping and Trap Filling in Organic Semiconductor Host-Guest Systems. *J. Phys. Chem. C* **2017**, *121*, 7767−7775.

(9) Arkhipov, V. I.; Heremans, P.; Emelianova, E. V.; Bassler, H. Effect of doping on the density-of-states distribution and carrier hopping in disordered organic semiconductors. *Phys. Rev. B: Condens. Matter Mater. Phys.* **2005**, *71*, 045214.

(10) Kurpiers, J.; Neher, D. Dispersive Non-Geminate Recombination in an Amorphous Polymer: Fullerene Blend. *Sci. Rep.* **2016**, *6*, 26832.

(11) Kim, G.; Pipe, K. P. Thermoelectric model to characterize carrier transport in organic semiconductors. *Phys. Rev. B: Condens. Matter Mater. Phys.* **2012**, *86*, 085208.

(12) Zuo, G. Z.; Abdalla, H.; Kemerink, M. Impact of doping on the density of states and the mobility in organic semiconductors. *Phys. Rev. B: Condens. Matter Mater. Phys.* **2016**, *93*, 235203.

(13) Chen, J.; Heeger, A. J.; Wudl, F. Confined Soliton Pairs (Bipolarons) in Polythiophene - Insitu Magnetic-Resonance Measurements. *Solid State Commun.* **1986**, *58*, 251−257.

(14) Wang, S.; Ha, M.; Manno, M.; Daniel Frisbie, C.; Leighton, C. Hopping transport and the Hall effect near the insulator-metal transition in electrochemically gated poly(3-hexylthiophene) transistors. *Nat. Commun.* **2012**, *3*, 1210.

(15) Sirringhaus, H. 25th Anniversary Article: Organic Field-Effect Transistors: The Path Beyond Amorphous Silicon. *Adv. Mater.* **2014**, *26*, 1319−1335.

(16) Venkateshvaran, D.; Nikolka, M.; Sadhanala, A.; Lemaur, V.; Zelazny, M.; Kepa, M.; Hurhangee, M.; Kronemeijer, A. J.; Pecunia, V.; Nasrallah, I.; Romanov, I.; Broch, K.; McCulloch, I.; Emin, D.; Olivier, Y.; Cornil, J.; Beljonne, D.; Sirringhaus, H. Approaching disorder-free transport in high-mobility conjugated polymers. *Nature* **2014**, *515*, 384−388.

(17) Khodagholy, D.; Rivnay, J.; Sessolo, M.; Gurfinkel, M.; Leleux, P.; Jimison, L. H.; Stavrinidou, E.; Herve, T.; Sanaur, S.; Owens, R. M.; Malliaras, G. G. High transconductance organic electrochemical transistors. *Nat. Commun.* **2013**, *4*, 2133.

(18) Lee, K. H.; Kang, M. S.; Zhang, S. P.; Gu, Y. Y.; Lodge, T. P.; Frisbie, C. D. "Cut and Stick" Rubbery Ion Gels as High Capacitance Gate Dielectrics. *Adv. Mater.* **2012**, *24*, 4457−4462.

(19) Bubnova, O.; Berggren, M.; Crispin, X. Tuning the thermoelectric properties of conducting polymers in an electrochemical transistor. *J. Am. Chem. Soc.* **2012**, *134*, 16456−16459.

(20) Zhang, F. J.; Zang, Y. P.; Huang, D. Z.; Di, C. A.; Gao, X.; Sirringhaus, H. N.; Zhu, D. B. Modulated Thermoelectric Properties of Organic Semiconductors Using Field-Effect Transistors. *Adv. Funct. Mater.* **2015**, *25*, 3004−3012.

(21) Venkateshvaran, D.; Kronemeijer, A. J.; Moriarty, J.; Emin, D.; Sirringhaus, H. Field-effect modulated Seebeck coefficient measurements in an organic polymer using a microfabricated on-chip architecture. *APL Mater.* **2014**, *2*, 032102.

(22) McCulloch, I.; Heeney, M.; Bailey, C.; Genevicius, K.; MacDonald, I.; Shkunov, M.; Sparrowe, D.; Tierney, S.; Wagner, R.; Zhang, W. M.; Chabinyc, M. L.; Kline, R. J.; Mcgehee, M. D.; Toney, M. F. Liquid-crystalline semiconducting polymers with high charge-carrier mobility. *Nat. Mater.* **2006**, *5*, 328−333.

(23) Lee, M. J.; Gupta, D.; Zhao, N.; Heeney, M.; McCulloch, I.; Sirringhaus, H. Anisotropy of Charge Transport in a Uniaxially Aligned and Chain-Extended, High-Mobility, Conjugated Polymer Semiconductor. *Adv. Funct. Mater.* **2011**, *21*, 932−940.

(24) Lee, J.; Panzer, M. J.; He, Y. Y.; Lodge, T. P.; Frisbie, C. D. Ion gel gated polymer thin-film transistors. *J. Am. Chem. Soc.* **2007**, *129*, 4532−4533.

(25) Said, E.; Crispin, X.; Herlogsson, L.; Elhag, S.; Robinson, N. D.; Berggren, M. Polymer field-effect transistor gated via a poly(styrenesulfonic acid) thin film. *Appl. Phys. Lett.* **2006**, *89*, 143507.

(26) Herlogsson, L.; Crispin, X.; Robinson, N. D.; Sandberg, M.; Hagel, O. J.; Gustafsson, G.; Berggren, M. Low-voltage polymer field-effect transistors gated via a proton conductor. *Adv. Mater.* **2007**, *19*, 97−101.

(27) Lee, J.; Kaake, L. G.; Cho, J. H.; Zhu, X. Y.; Lodge, T. P.; Frisbie, C. D. Ion Gel-Gated Polymer Thin-Film Transistors: Operating Mechanism and Characterization of Gate Dielectric Capacitance, Switching Speed, and Stability. *J. Phys. Chem. C* **2009**, *113*, 8972−8981.

(28) Choi, J. H.; Xie, W.; Gu, Y. Y.; Frisbie, C. D.; Lodge, T. P. Single Ion Conducting, Polymerized Ionic Liquid Triblock Copolymer Films: High Capacitance Electrolyte Gates for n-type Transistors. *ACS Appl. Mater. Interfaces* **2015**, *7*, 7294−7302.

(29) Harada, T.; Ito, H.; Ando, Y.; Watanabe, S.; Tanaka, H.; Kuroda, S.-i. Signature of the insulator−metal transition of a semicrystalline conjugated polymer in ionic-liquid-gated transistors. *Appl. Phys. Express* **2015**, *8*, 021601.

(30) Cochran, J. E.; Junk, M. J. N.; Glaudell, A. M.; Miller, P. L.; Cowart, J. S.; Toney, M. F.; Hawker, C. J.; Chmelka, B. F.; Chabinyc, M. L. Molecular Interactions and Ordering in Electrically Doped Polymers: Blends of PBTTT and F(4)TCNQ. *Macromolecules* **2014**, *47*, 6836−6846.

(31) Egginger, M.; Irimia-Vladu, M.; Schwodiauer, R.; Tanda, A.; Frischauf, I.; Bauer, S.; Sariciftci, N. S. Mobile ionic impurities in poly(vinyl alcohol) gate dielectric: Possible source of the hysteresis in organic field-effect transistors. *Adv. Mater.* **2008**, *20*, 1018−1022.

(32) Glaudell, A. M.; Cochran, J. E.; Patel, S. N.; Chabinyc, M. L. Impact of the Doping Method on Conductivity and Thermopower in Semiconducting Polythiophenes. *Adv. Energy Mater.* **2015**, *5*, 1401072.

(33) Xuan, Y.; Liu, X.; Desbief, S.; Leclere, P.; Fahlman, M.; Lazzaroni, R.; Berggren, M.; Cornil, J.; Emin, D.; Crispin, X. Thermoelectric properties of conducting polymers: The case of poly(3-hexylthiophene). *Phys. Rev. B: Condens. Matter Mater. Phys.* **2010**, *82*, 115454.

(34) Kang, S. D.; Snyder, G. J. Charge-transport model for conducting polymers. *Nat. Mater.* **2017**, *16*, 252−257.

(35) DeLongchamp, D. M.; Kline, R. J.; Lin, E. K.; Fischer, D. A.; Richter, L. J.; Lucas, L. A.; Heeney, M.; McCulloch, I.; Northrup, J. E. High carrier mobility polythiophene thin films: Structure determination by experiment and theory. *Adv. Mater.* **2007**, *19*, 833−837.

(36) Northrup, J. E. Atomic and electronic structure of polymer organic semiconductors: P3HT, PQT, and PBTTT. *Phys. Rev. B: Condens. Matter Mater. Phys.* **2007**, *76*, 245202.

(37) Noriega, R.; Rivnay, J.; Vandewal, K.; Koch, F. P. V.; Stingelin, N.; Smith, P.; Toney, M. F.; Salleo, A. A general relationship between disorder, aggregation and charge transport in conjugated polymers. *Nat. Mater.* **2013**, *12*, 1038−1044.

DOI: 10.1021/acs.chemmater.8b00394
Chem. Mater. 2018, 30, 2965−2972

(38) Cohen, M. H.; Economou, E. N.; Soukoulis, C. M. Microscopic Mobility. *Phys. Rev. B: Condens. Matter Mater. Phys.* **1984**, *30*, 4493−4550.
(39) Rivnay, J.; Noriega, R.; Northrup, J. E.; Kline, R. J.; Toney, M. F.; Salleo, A. Structural origin of gap states in semicrystalline polymers and the implications for charge transport. *Phys. Rev. B: Condens. Matter Mater. Phys.* **2011**, *83*, 121306R.
(40) Abdalla, H.; Zuo, G. Z.; Kemerink, M. Range and energetics of charge hopping in organic semiconductors. *Phys. Rev. B: Condens. Matter Mater. Phys.* **2017**, *96*, 241262R.
(41) Chew, A. R.; Salleo, A. Spectroscopic studies of dopant-induced conformational changes in poly (3-hexylthiophene) thin films. *MRS Commun.* **2017**, *7*, 728−734.
(42) Tashiro, K.; Kobayashi, M.; Kawai, T.; Yoshino, K. Crystal structural change in poly(3-alkyl thiophene)s induced by iodine doping as studied by an organized combination of X-ray diffraction, infrared/Raman spectroscopy and computer simulation techniques. *Polymer* **1997**, *38*, 2867−2879.
(43) Hynynen, J.; Kiefer, D.; Yu, L. Y.; Kroon, R.; Munir, R.; Amassian, A.; Kemerink, M.; Muller, C. Enhanced Electrical Conductivity of Molecularly p-Doped Poly(3-hexylthiophene) through Understanding the Correlation with Solid-State Order. *Macromolecules* **2017**, *50*, 8140−8148.
(44) Hulea, I. N.; Brom, H. B.; Houtepen, A. J.; Vanmaekelbergh, D.; Kelly, J. J.; Meulenkamp, E. A. Wide energy-window view on the density of states and hole mobility in poly(p-phenylene vinylene). *Phys. Rev. Lett.* **2004**, *93*, 166601.
(45) Pingel, P.; Neher, D. Comprehensive picture of p-type doping of P3HT with the molecular acceptor F(4)TCNQ. *Phys. Rev. B: Condens. Matter Mater. Phys.* **2013**, *87*, 115209.
(46) Giovannitti, A.; Sbircea, D. T.; Inal, S.; Nielsen, C. B.; Bandiello, E.; Hanifi, D. A.; Sessolo, M.; Malliaras, G. G.; McCulloch, I.; Rivnay, J. Controlling the mode of operation of organic transistors through side-chain engineering. *Proc. Natl. Acad. Sci. U. S. A.* **2016**, *113*, 12017−12022.
(47) Friedlein, J. T.; Rivnay, J.; Dunlap, D. H.; McCulloch, I.; Shaheen, S. E.; McLeod, R. R.; Malliaras, G. G. Influence of disorder on transfer characteristics of organic electrochemical transistors. *Appl. Phys. Lett.* **2017**, *111*, 023301.
(48) McCulloch, I.; Heeney, M.; Bailey, C.; Genevicius, K.; JacDonald, I.; Shkunov, M.; Sparrowe, D.; Tierney, S.; Wagner, R.; Zhang, W.; Chabinyc, M. L.; Kline, R. J.; McGehee, M. D.; Toney, M. F. Liquid-crystalline semiconducting polymers with high charge-carrier mobility. *Nat. Mater.* **2006**, *5*, 328−333.

DOI: 10.1021/acs.chemmater.8b00394
Chem. Mater. 2018, 30, 2965−2972